XVII European Conference
ECSMGE 2019
Reykjavík
on Soil Mechanics
and Geotechnical Engineering

Analysis of the failure mode of slopes with open sharp toe notches
Analyse du mode de rupture des pentes à crans ouverts

Luis E. Vallejo
Department of Civil Engineering, University of Pittsburgh, Pittsburgh, USA

Mingzhou Li
Department of Civil Engineering, University of Pittsburgh, Pittsburgh, USA

ABSTRACT: A notch (or toe crack with an open angle) in coastal and inland slopes is one of the primary factors responsible for their failure. For the case of coastal slopes, the open notch at the toe of slopes is caused by the erosion of the toe material by wave action. For the case of inland slopes, the open notch is produced by the combination of water-induced slaking of the material at the toe of the slopes and the expansion of the face of the slope resulting from the stress relaxation that takes place when a cut is made in soil or rock. This study describes the mechanics of formation of open notches in coastal and inland slopes which are located in England and the United States. An open notch in a slope acts as stress concentrator. If a slope with an open notch fails, the failure starts at the tip of the open notch where the stresses are the highest. Thus, a notch dictates the way the slopes fail. An explanation for the influence of sharp open notches on the stability of rock and soil slopes is presented. The sharp notches considered had varying degrees in the angle formed by the walls of the open sharp notch. The stability analysis used the results of laboratory, numerical (FEM) and theoretical analysis. The theoretical analysis was based on Linear Elastic Fracture Mechanics theory.

RÉSUMÉ: Une entaille (ou une fissure à l'angle ouvert) sur les pentes côtières et intérieures est l'un des principaux facteurs responsables de leur défaillance. Dans le cas des pentes côtières, l'entaille ouverte au pied des pentes est provoquée par l'érosion du matériau de la pointe par l'action des vagues. Dans le cas de pentes intérieures, l'entaille ouverte est produite par la combinaison de l'extinction du matériau induite par l'eau au pied des pentes et de l'élargissement de la surface de la pente résultant de la relaxation des contraintes qui se produit lors de la coupe fait dans le sol ou la roche. Cette étude décrit les mécanismes de formation des entailles ouvertes dans les pentes côtières et intérieures situées en Angleterre et aux États-Unis. Une encoche ouverte dans une pente sert de concentrateur de contraintes. Si une pente avec une encoche ouverte échoue, l'échec commence au bout de l'encoche ouverte où les contraintes sont les plus élevées. Ainsi, une entaille détermine la manière dont les pentes échouent. Une explication de l'influence des entailles ouvertes et nettes sur la stabilité des pentes de roche et de sol est présentée. Les encoches tranchantes considérées avaient des degrés variables dans l'angle formé par les parois de l'entaille tranchante ouverte. L'analyse de stabilité a utilisé les résultats d'analyses de laboratoire, numériques (FEM) et théoriques. L'analyse théorique était basée sur la théorie de la mécanique de fracture élastique linéaire.

Keywords: Notches; coastal slopes; crack propagation; finite element; linear elastic fracture mechanics.

1 INTRODUCTION

Investigations were carried out to study the mechanics of notch formation in soil slopes forming part of the shorelines in England and inland slopes in the United States. The influence of the notch (a wave induced cut in the soil or rock) on the stability of these slopes was also analyzed using field, theoretical and numerical analyses.

The selected soil slopes are located at Aldbrough on the north east coast of England and Vicksburg, Mississippi in the U.S (Hutchinson, 1986, 1988; Lutton, 1969). Also, a laboratory soil slope with a toe crack was tested in the laboratory. Figures 1 through 3 shows the notches in the soil slopes and the laboratory soil slope.
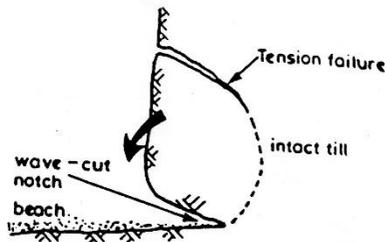

Figure 1. A wave induced notch in a till coastal slope located at Aldbrough on the coast of England (Hutchinson, 1986, 1988).

The slope shown in Figure 1 is located in the Holderness coast in the north east part of England. The height of the slope is about 3 meters, and its inclination is about 65 degrees. The slope is made of the Holderness till (Hutchinson, 1986, 1988). The slope in Fig. 2 is made of loess. Its height is about 10 meters and
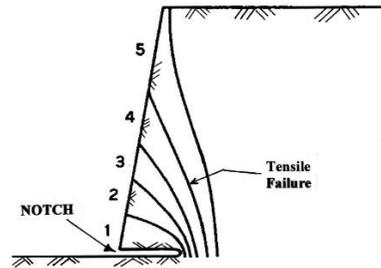

Figure 2. Progression of toe failures from an open notch in a soil slope located at Vicksburg, Mississippi (Lutton, 1969).
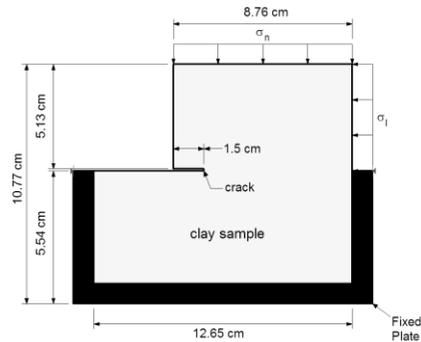

Figure 3. A clay slope with an open crack at its toe for testing in the PSDSA.

its face is inclined at 70 degrees with the horizontal (Lutton, 1969).

2 NOTCH INDUCED FAILURE OF THE SLOPES

2.1 Notch induced failure of the soil slopes

The notches and the failure surfaces in the soil slope shown in Figure 1 was the result of wave action at their toes (Figure 4)(Vallejo and DeGroot, 1988). The action of the ocean water waves on this coastal slope consists primarily of

the erosion of previously intact soil occupying the slope foot and adjacent to the wave-cut platform. The erosion takes the form of wave impact and abrasion. The net result of the wave erosion is the formation of a notch at the foot of the coastal slope. The notches shown in Figure 1 act as stress concentrator and causes the tensile failure of the material surrounding the notch
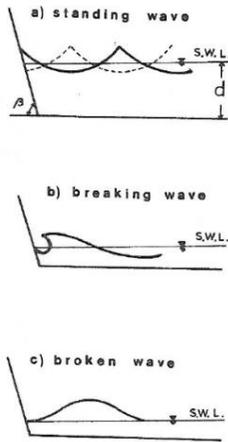

Figure 4. Different wave types acting at the toe of coastal slopes.

For the case of the loess slope shown in Figure 2, the notch was produced by the water induced slaking of the loess. After rain, water accumulates at the toe of the slope resulting on the slaking of the slopes' toe material (Vallejo, 2011). Like in the coastal slopes, the notch acts as stress concentrator that causes the tensile failure of the slope as shown in Figure 2.

2.2 Laboratory soil slope with a toe crack

To create a soil slope with a toe crack, kaolinite clay was chosen as the soil material because it forms a homogeneous material which minimizes the adverse effects of micro-scale heterogeneities. Kaolinite used for this research

exhibited a liquid limit = 58%, plastic limit = 28%, and plasticity index = 30%.

Prepared soil samples were placed in an circular oedometer with 30 cm in diameter and consolidated under a normal pressure of 25.7 kPa for a period of 5 days. After unloading the oedometer, prismatic samples were then cut that measured 12.65 cm in length, 8.25 cm in height and 2.54 cm in thickness. The water content of the samples were at or slightly above the plastic limit (w=30%) after removal from the oedometer. After this was done, the clay sample with with dimension shown in Fig. 3 was prepared for testing in the Plane Stress Diret Shear Apparatus (PSDSA) (Vallejo, 1991).

Fig. 3 represents a simulated vertical slope with an artificial horizontal open crack at the toe of slope. The clay slope simulated a slope with a vertical face. Figure 3 presents the dimensions of the clay slope model and Fig. 5 shows the actual laboratory sample with the original horizontal crack that measured 1.5 cm in length before [Fig. 5(a)] and after the test [Fig. 5(b)]. The applied normal stress (σ_n) simulates the gravity stress acting on the slope and the lateral stress (σ_l) simulates the lateral earth pressure (Fig. 3). Both of these stresses can be applied by the PSDSA. When the sample was ready to be tested in the PSDSA, the water content in the sample, w, was equal to 10%.
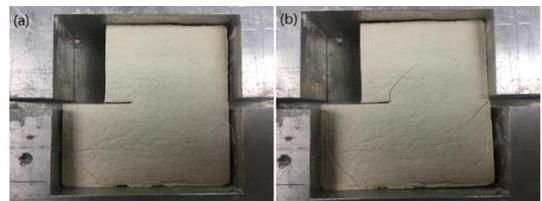

Figure 5. (a) The fissured clay sample before testing, and (b) after testing in the PSDSA.

A normal stress (σ_n) of 513 kPa was applied to the sample with an open toe crack. The normal stress was kept constant during the experiment. The lateral stress (σ_l) induced a

shear stress, τ , on the solid horizonal section of the crack [Fig. 5(a)]. The lateral stress (σ_l) was gradually increased until the toe crack began to propagate, which occurred when the shear stress τ = 513 kPa [Fig. 5(b)]. The toe crack propagated in the model in the form of a secondary crack that extend from the toe of the pre-existing crack and deviated from the original horizontal direction. Figure 5(b) shows the clay model after the test. The secondary tensile crack propagated at an average angle of 80^0 with the direction of the pre-existing horizontal crack.

3 ANALYSIS OF THE NOTCH FAILURES USING FRACTURE MECHANICS THEORY

3.1 Stresses at the notch of the slopes

The stresses on an element near the tip of a notch in a coastal slope are: a tangential stress σ_θ, a radial stress σ_r, and a shear stress $\tau_{r\theta}$ (Fig. 6). Of these three stresses, the tangential stress causes the failure of the intact material and is directly responsible for the propagation of the notch in the form of a secondary tensile crack (failure surface) that starts from the tip of the notch. The secondary tensile crack follows the direction of r which is normal to the tangential stress σ_θ and is inclined at an angle θ with the axis X (Vallejo , 1994). According to Vallejo (1994), the tangential stress σ_θ can be obtained from the following relationship that uses Fracture Mechanics theory,

$$\sigma_\theta = \frac{1}{\sqrt{2\pi r}} \cos\frac{\theta}{2}(K_I \cos^2\frac{\theta}{2} - \frac{3}{2} K_{II} \sin\theta) \quad (1)$$

In the above equation, K_I and K_{II} are the stress intensity factors. The value of these stress intensity factors can be obtained from the following relationships (Vallejo, 1994).
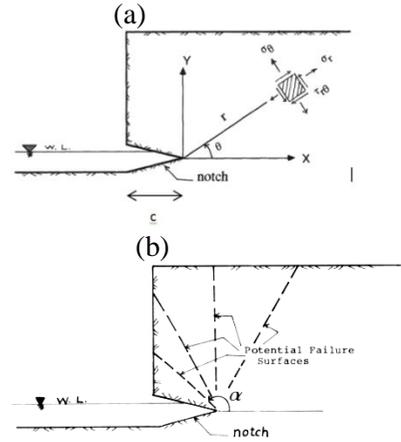

Figure 6. (a) Stresses in the intact material near the tip of a notch; (b) Angles of secondary cracks

$$K_I = 1.12\ \sigma_n(\pi c)^{1/2} \quad (2)$$

and

$$K_{II} = 1.12\ \tau(\pi c)^{1/2} \quad (3)$$

where σ_n is the normal (overburden) stress that acts perpendicular to the horizontal axis X of the notch, τ is the shear stress (resulting from the lateral earth pressure) that acts parallel to the horizontal axis X of the notch, and c is the notch length (Fig. 6).

3.2 Angle of crack propagation from the notches using Fracture Mechanics theory

The notch in the slope shown in Figure 6(a) propagates following the direction r. This propagation takes place when the value of σ_θ reaches its maximum value at a certain value of θ = α [Figure 6(b)]. To obtain the direction of θ = α at which σ_θ reaches its maximum value, one

only needs to differentiate σ_θ with respect to θ and make the whole differentiation equal to zero ($d\sigma_\theta d\theta = 0$). If this is done the following relationship is obtained from which the angle α can be obtained,

$$\sin\alpha + \left(\frac{K_{II}}{K_I}\right)(3\cos\alpha - 1) = 0 \qquad (4)$$

Using Equation (4) and Equations (2) and (3), a plot between the angle of crack propagation α and the ratio (K_{II}/K_I) or (τ/σ_n) can be obtained and is shown in Figures 7 and 8. Figure 7 shows that the angle of secondary crack propagation from the tip of the notch (Fig. 6) for any value of the ratio τ/σ (or K_{II}/K_I). Figure 8 shows the angle of secondary crack propagation for values of τ/σ (or K_{II}/K_I) between 0 and 1.
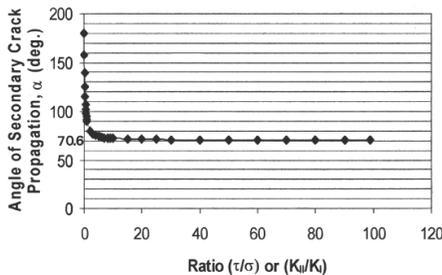

Figure 7. Angle of secondary crack propagation for any value of the ratio (τ/σ) or (K_{II}/K_I)
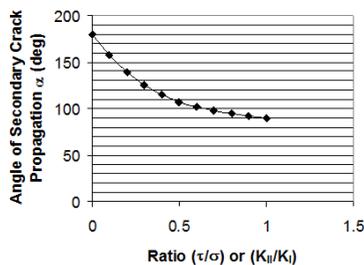

Figure 8. Angle of secondary crack propagation for any value of the ratio (τ/σ) or (K_{II}/K_I) between 0 and 1.

3.3 Calculation of the angle of crack propagation in the field and in the laboratory using results Fracture Mchanics Theory

For the case of the case of the slope shown in Figure 2, the notch was produced by the water induced slaking of the loess. After rain, water accumulates at the toe of the slope resulting on the slaking of the slopes' toe material (Vallejo, 2011). For the case of the soil slope shown in Figure 2, the first tensile failure surface was inclined at about $\alpha = 160^0$ in a counter clockwise direction with respect to the horizontal [Fig. 6(b)]. The second failure surface was inclined at about 130^0. The subsequent failure surfaces took place at smaller angles than the first two. The notch shown in Figure 2 acts as stress concentrator that causes the tensile failure of the slope. The soil slope in Figure 1 also failed when a tensile crack inclined at an angle $\alpha > 90^0$.

For the case of the laboratory slope the angle of seconadry crack α was equal to 80°. For a ratio between τ/σ equal to 6.3. For this ratio, the theoretical value of α given by Fig. 8 is about 80°.

Thus, the angles of secondary crack propagation in the field and laboratory samples seem to be predicted well by the principles of Fracture Mechanics given by Fig. 8. This Figure shows that the angle of secondary crack propagation, α, for ratios τ/σ less than 1, goes from 90^0 to 180^0 (Fig. 8). These angles of secondary crack propagation were effective in the slopes in the field (Figures 1, and 2). For ratios τ/σ more than 1 , the angles of crack propagation varies between 90° and 70.6° (Fig. 7).

4 ANGLE OF CRACK PROPAGATION USING FINITE ELEMENT METHOD

The angle of crack propagation of slopes subjected to the type of stresses presented in Fig. 4 was also calculated using the ABAQUS

(2006)) finite element method. The properities of the naterias used are shown in Table 1. The model used for the finite element method is shown in Fig. 3. The sample is fixed at the lower plate. The results of this analysis is shown in Figs. 9 to 11 for different values of the ratio τ/σ.

Table 1. Material properties values for the FEM

Property	Value
Young's modulus of Elasticity, E	0.56 MPa
Poisson's ratio	0.3
Density, ρ	2000 kg/m^3

4.1 Results of finete element analysis

The results of the finite element analysis is shown in Figs. 9, 10 , and 11 for different values of the ratio τ/σ .
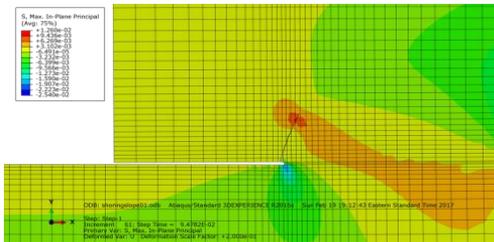

Figure 9. Plot of maximum stresses (+ is tension) and crack propagation for $\tau/\sigma_n > 1$
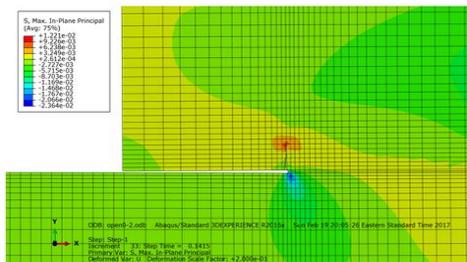

Figure 10. Plot of maximum stresses (+ is tension) and crack propagation for $\tau/\sigma_n = 1$
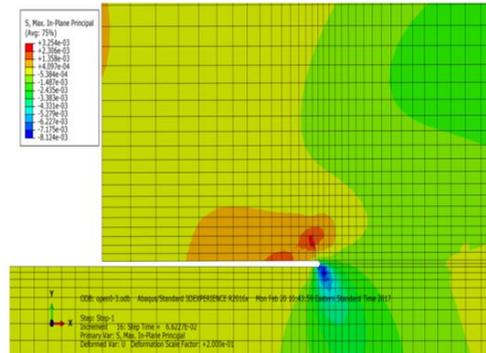

Figure 11. Plot of maximum stresses (+ is tension) and crack propagation for $\tau/\sigma_n < 1$

The angle of crack propagation α depicted in Figs. 9 to 11 are equal to 62º, 88º, and 115º. These angles are measured in a counter clockwise direction with respect to the axis X shown in Fig. 6.

The results of the FEM analysis also substantiates the results on the angle of crack propagation in the slopes in the field (Figs. 1 and 2) as well the results of the laboratory tests (Fig. 5).

5   CONCLUSIONS

The present study has presented examples of notches in coastal and inland slopes made of soil. For the case of coastal slopes, notches are the result of wave action. For the case of inland soil slopes, notches are the result of slaking The notches that were open or were found to act as stress concentrators. Notches caused the tensile failure of the slopes. The tensile failures were the result of secondary tensile cracks that started at the tip of the notches and propagated inside the slope. The angle of propagation of the secondary cracks was evaluated using laboratory studies, the principles of linear elastic Fracture Mechanics theory, and finite element analysis. It was determined that the inclination of the tensile secondary cracks in the slopes in the field and in

the laboratory, were predicted very well by linear elastic Fracture Mechanics theory and numerical analysis such as the finite element method.

6   REFERENCES

ABAQUS 2006. *User's Manual Version 6.6.* Simulia, Providence, R.I.

Hutchinson, J.N. 1986. Cliffs and shores in cohesive materials: geotechnical and engineering geological aspects. *Proceedings Symposium on Cohesive Shores.* Burlington, Ontario, pp. 1-44.

Hutchinson, J.N. 1988. General report: morphological and geotechnical parameters in land slides in relation to geology and hydrology. *Proceedings of the 5th Int. Symposium on Landslides*, Lausanne, 1: 3-35.

Lutton, R.J. 1969. *Fracture and Failure Mechanisms in Loess and Applications to Rock Mechanics.* U.S. Army Corps of Engineers, Report S-69-1.

Vallejo, L.E. 1991. A Plane Stress Direct Shear Apparatus for testing clays. *Geotechnical Special Publication, ASCE,* 27: 851-862.

Vallejo, L.E. 2011. Mechanics of the slaking of shales. *Geomechanics and Engineering*, 3: 219-231.

Vallejo, L.E. and DeGroot, R. 1988. Bluff response to wave action. *Engineering Geology,* 26: 1-16.

Vallejo, L.E., 1994. Application of Fracture Mechanics to soils. *Geotechnical Special Publication*, ASCE, 43:1-20.